Supplementary information

Magnetic Field Assisted Assembly of Highly Ordered Percolated Nanostructures and Their Application for Transparent Conductive Thin Films

Oleksandr Trotsenko,[a] Alexander Tokarev,[a] Alexey Gruzd,[a] Timothy Enright[a] and Sergiy Minko*[a]

[a]Nanostructured Materials Laboratory, the University of Georgia, Athens, GA 30602, United States, E-mail: sminko@uga.edu

S1. Percolating structures and percolation threshold

Thin films of conductive nanowires have regions when some fraction of the conductive material is excluded from the conductive network due to different defects including poor electrical contacts between nanowires, and typical defects of the network structure such as dangling ends and loops. The defective regions are experimentally demonstrated in **Fig. S1** when topographical atomic force microscopy (AFM) images (a and c) are compared with electrical conductivity AFM imaging (b and d). Some wires and fragments of the network that are imaged with the topographical contrast are invisible in the conductivity images representing a fraction of wires that are not included in the percolated conducting structures.

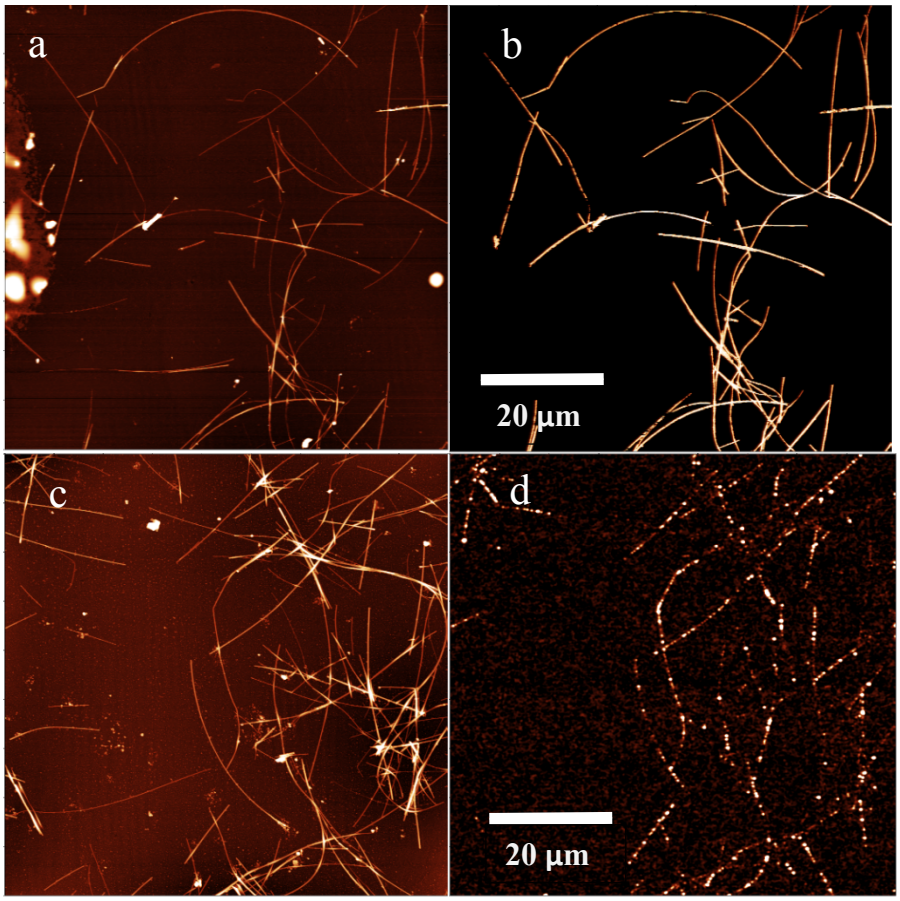

Fig. S1**.** Nanoelectrical imaging of randomly deposited silver nanowires. AFM images of topography (a and c) and TUNA current (b and d). Using PeakForce TUNA mode a bias of 500 mV (b) and 9V (d) was applied between conductive probe and the sample. A higher bias voltage was needed for the area in the middle of sample (c) comparing to the area near the edge (a) close to the contact with the stage. The highlighted regions show TUNA current between the probe and the short path of silver nanowires in the percolating network. Some of wires are isolated from the percolating network and, thus, are not visible on the TUNA image. Z scale is 250 nm for topography images (a and c), 120 nA and 20 pA for TUNA current images (b and d), respectively.

Magnetically deposited two layer networks of nanowires can be described using an *idealized 2D Archimedean square lattice*[1] with fragments (bonds of a length *l* and a diameter *d*) when each end is in contact with 3 other lattice fragments. A number of fragments *N* is in the area L^2; a number of fragments in the fully occupied network is $N_m = 2(L/l)^2+2(L/l)$. Fragment percolation threshold for this model is 0.5 or in other words a half of all the grid fragments are needed for percolation which is $N_c = (L/l)^2+(L/l)$. The fraction of the area covered with fragments at percolation is $N_c ld/L^2=d/l + d/L$. For the dimensions of the nanowires used in this work *l* = 25 µm and *d*= 90 nm, the calculated critical fraction area of nanowires for percolation is 0.36%. Furthermore, a maximum concentration of nanowires in a

single layer of 100% densely packed nanowires in area $L^2 = 1\ m^2$ can be calculated as $\rho_{Ag}\pi dL^2/4 = 741\ mg/m^2$, where ρ_{Ag} is the density of Silver. Considering maximum nanowire density value, nanowire coating with the percolation fraction area of nanowires 0.36% has a nanowire concentration density of $3\ mg/m^2$, which is the percolation concentration of nanowires in 2D Archimedean square lattice. *Isotropic coatings* were modeled as 2D random networks of high aspect ratio rectangles[2] when $N_C L^2 = 5.504$. This model estimated the critical fraction area as $N_c ld/L^2$ = 2.75%, which corresponds to a critical nanowires density of 20 mg/m^2.

Using the estimations we fitted the experimental resistivity data (inset Figure 2a) for the aligned (N_c =12 mg/m^2) and random networks (N_c =20 mg/m^2), respectively. Slopes k of the linear fit are values for percolation critical exponent with negative sign. The critical exponents and N_c percolation densities were used to fit the experimental relationship of resistance vs. surface density (Figure 2a). Our experimental measurements are given in terms of sheet resistance (R_{sh}) which is inversely proportional to the conductivity ($\sigma \propto 1/ R_{sh}$) and weight concentration of nanowires per unit area (ρ), where number of wires per unit area N = kρ.

Thus, $1/R_{sh} \propto \sigma \propto (N - N_c)^t = k^t (\rho - \rho_c)^t$

and $R_{sh} \propto (\rho - \rho_c)^{-t}$

S2.Experimental setup and characteristics of the magnet

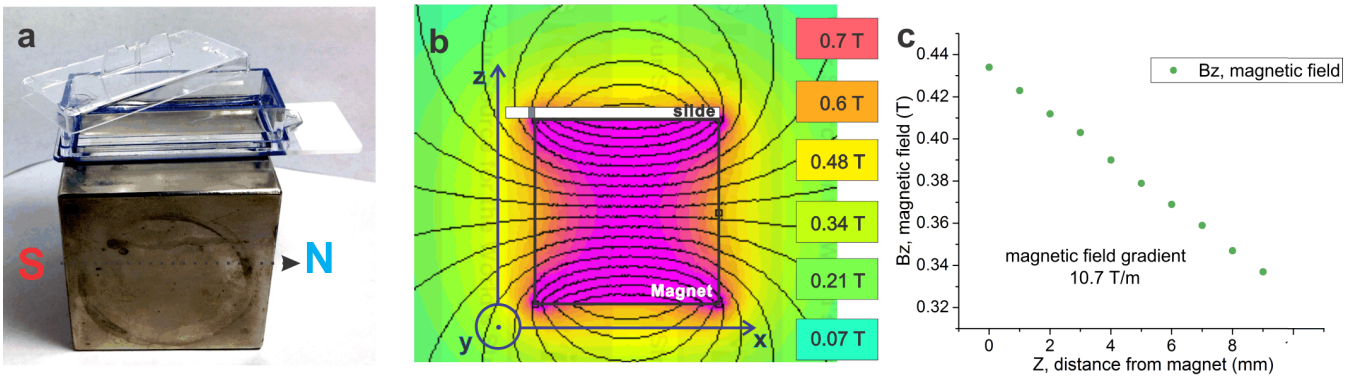

Fig. S2. (a) Experimental setup for the cubic NdFeB magnet (Grade N42 by K&J Magnetics, Pipersville, PA) with dimensions 2 x 2 x 2 inches. (b) Black square schematically shows the location of a glass slide with working area of 1 x 2 inches placed on the magnet parallel to the magnetization direction. Color bar denotes magnetic field in Tesla units. (c) Strength of the magnetic field B_z in Z direction

calculated for middle point on the sample. Magnetic field gradient close to the magnet surface is 10.7 T/m.

The experimental setup that includes the glass cuvette with the cover and the rectangular magnet under the cuvette is shown in **Fig. S2a**. The experimental characteristics of the magnetic field acting on the nanowires are shown in **Fig.S2b and c**.

S3. AFM band SEM imaging of the silver wire networks at different conditions

AFM images of the nanowires decorated with magnetic nanoparticles aligned in one and two orthogonal directions are shown in AFM images **Fig. S3** a, b and c, respectively. AFM topography images (**Fig. S4a**) and SEM image (**Fig. S4b**) of randomly deposited silver nanowires decorated with PEI coated magnetite nanoparticles in magnetic field with low tangential and strong normal component are shown in Fig. S4. The wire network on a flexible substrate (a carbon tape) after deformations (bending) is shown in **Fig. S5a**. Silver nanowires after etching examined with SEM, show no residual iron oxide particles and a very small fraction of silvers spherical particles (Fig. S4, b,c).

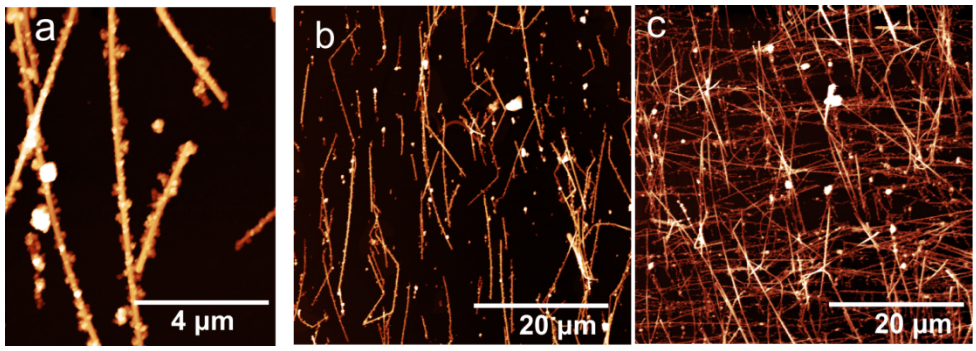

Fig. S3. (a) AFM topography images of silver nanowires decorated with PEI coated magnetite nanoparticles,(b) aligned in one and (c) two directions. Magnetite nanoparticles were not etched and can be observed on the nanowires and on the substrate.

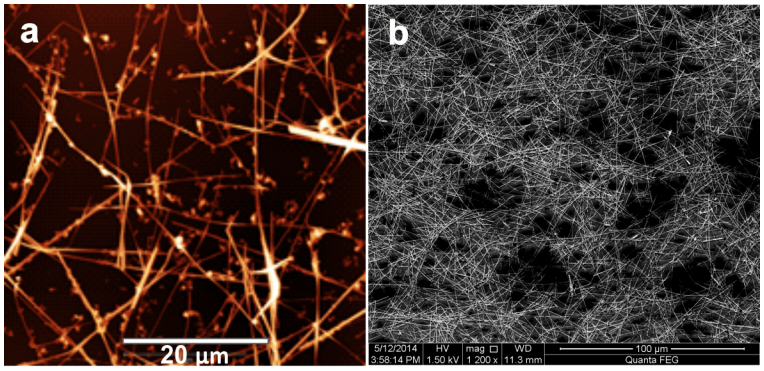

Fig. S4. (a) AFM topography image and (b) SEM image of randomly deposited silver nanowires decorated with PEI coated magnetite nanoparticles in magnetic field with a low tangential and a strong normal component.

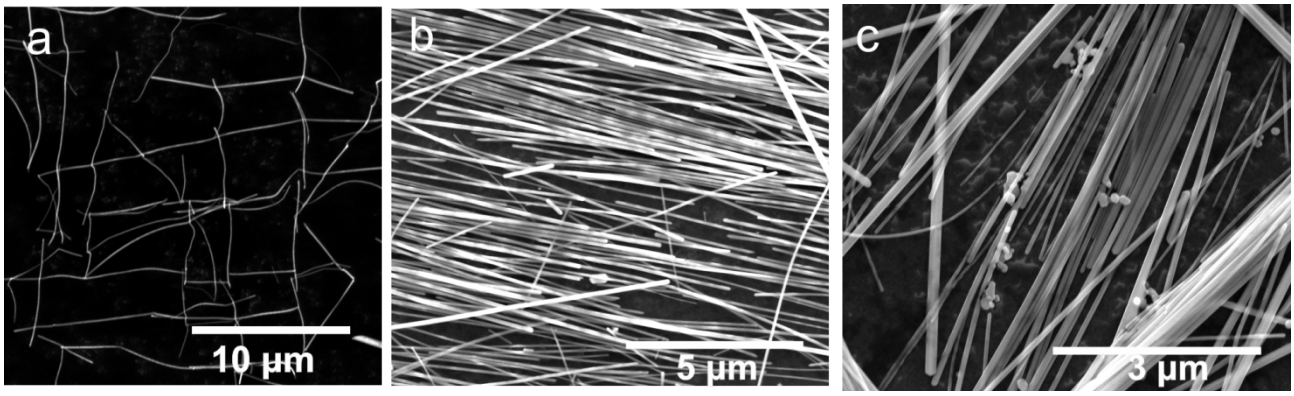

Fig. S5. SEM images of (a) annealed magnetically aligned silver nanowires networks transferred to carbon tape; the network is deformed but ordered; (b) densely packed aligned silver nanowires deposited in magnetic field with etched magnetite nanoparticles; (c) small fraction of silver nanoparticles were found along with silver nanowires.

S4. Characteristics of the magnetic particles (MNP) coated with PEI and silver nanowires (SNW)

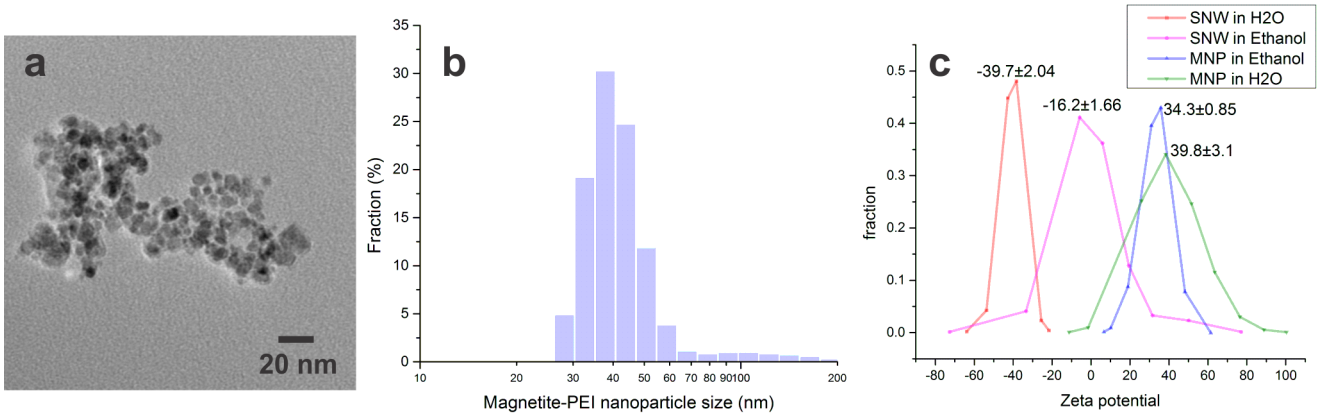

Fig. S6. (a) TEM image of magnetite nanoparticles coated with PEI. (b)DLS size distribution of magnetite nanoparticles coated with PEI; (c) Zeta-potential of magnetic nanoparticles and silver nanowires at pH6.

S5. Kinetics of magnetophoretic deposition of silver nanowires in cuvette

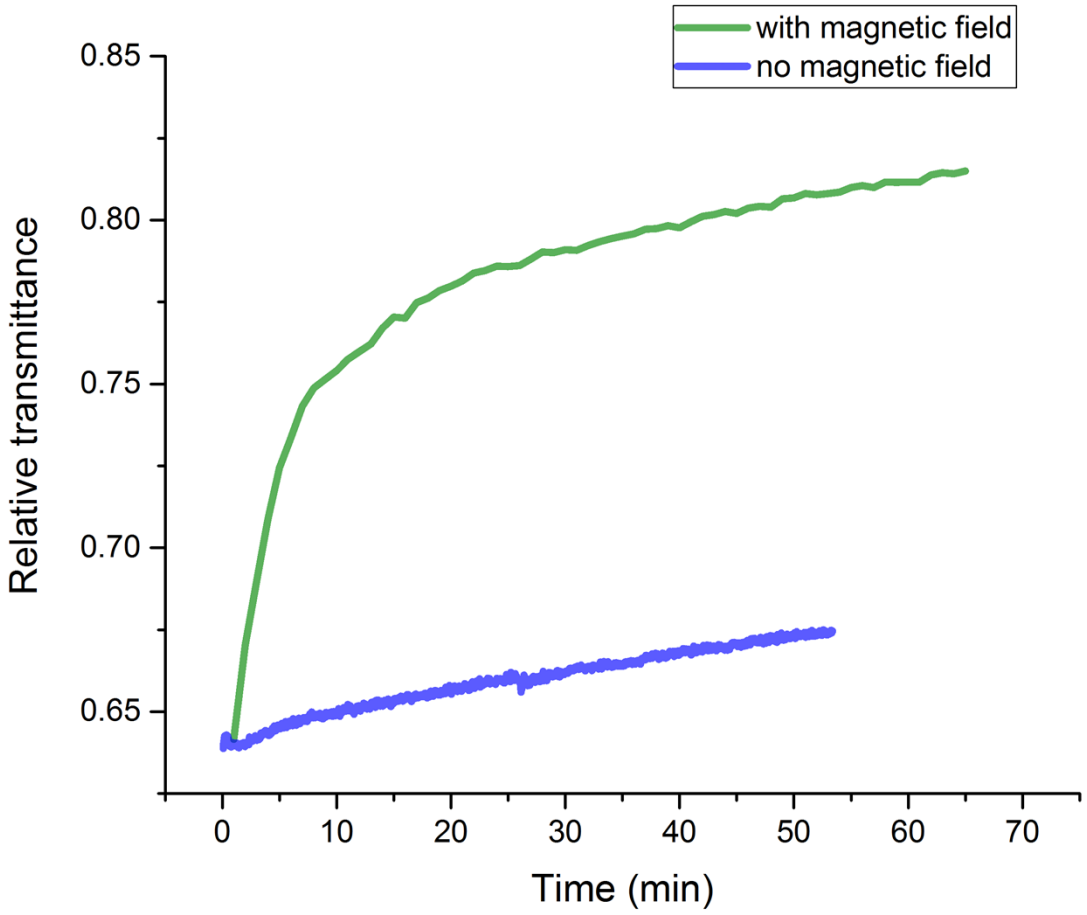

Fig. S7 Kinetics of the deposition of silver nanowires coated with magnetic nanoparticles with and without magnetic field. Measurements are relative intensity of the light transmitted through the polystyrene cuvette with mixture of 0.01% silver nanowires and 0.01% magnetic nanoparticles in ethanol. Data on the plots shows intensity of a light beam passing the cuvette 7.5 mm above the magnet surface.

References

1. P. N. Suding, R. M. Ziff, Physical Review E 1999, 60, 275-283.

2. J. Li, M. Östling, Physical Review E 2013, 88, 012101.